ZnO Nanotips Grown on Si Substrates by Metal-Organic Chemical-Vapor Deposition

J. ZHONG,[1] S. MUTHUKUMAR,[2] G. SARAF,[1] H. CHEN,[1] Y. CHEN,[1] and Y. LU[1,3]

1.—Department of Electrical and Computer Engineering, Rutgers University, Piscataway, NJ 08854. 2.—Department of Ceramic and Materials Engineering, Rutgers University, Piscataway, NJ 08854. 3.—E-mail: ylu@ece.rutgers.edu

The ZnO nanotips are grown on silicon and silicon-on-sapphire (SOS) substrates using the metal-organic chemical-vapor deposition (MOCVD) technique. The ZnO nanotips are found to be single crystal and vertically aligned along the c-axis. In-situ Ga doping is carried out during the MOCVD growth. The ZnO nanotips display strong near-band edge photoluminescence (PL) emission with negligible deep-level emission. Free excitonic emission dominates the 77-K PL spectrum of the as-grown, undoped ZnO nanotips, indicating good optical properties and a low defect concentration of the nanotips. The increase of PL intensity from Ga doping is attributed to Ga-related impurity band emission. Photoluminescence quenching is also observed because of heavy Ga doping. ZnO nanotips grown on Si can be patterned through photolithography and etching processes, providing the potential for integrating ZnO nanotip arrays with Si devices.

Key words: ZnO, metal-organic chemical-vapor deposition (MOCVD), silicon-on-sapphire (SOS), nanostructure, photoluminescence (PL)

INTRODUCTION

Nanowires and nanotips are the key functional components for nanoscale electronic and photonic devices.[1] Zinc oxide is a direct wide bandgap semiconductor with a high exciton-binding energy of 60 meV. Enhanced carrier and photon confinement in ZnO nanowires have been exploited to demonstrate an optically pumped, low-threshold ultraviolet nanolaser at room temperature.[2] A variety of techniques have been employed to grow ZnO nanowires, such as vapor-phase transport,[2] catalyst-assisted molecular-beam epitaxy,[3] chemical-vapor deposition,[4] and metal-organic chemical-vapor deposition (MOCVD).[5,6] Among these methods, MOCVD provides the capability of mass production and controllable in-situ doping. Its low growth temperature is preferred for device integration using mainstream semiconductor-processing technologies. ZnO nanotips have been selectively grown on various substrates.[6] ZnO nanowires grown on c-sapphire by metal-organic vapor-phase epitaxy have shown promising optical properties with a free excitonic emission at 10 K.[5]

Nanotips grown on Si substrates are of strong interest because of potential integration with the well-developed Si-processing technology. However, ZnO nanowires synthesized on Si substrates in a widely used vapor-liquid-solid (VLS) process are randomly oriented.[7,8] The VLS growth leads to incorporation of metallic impurities in the as-grown ZnO nanowires. There are few reports on aligned ZnO nanotips grown on Si substrates via MOCVD.[6,9] In particular, ZnO nanotips grown on silicon-on-sapphire (SOS) substrates open up the possibility to directly integrate ZnO one-dimensional (1-D) nanostructures, ZnO epitaxial layers, and Si-based electronic devices on one chip. Furthermore, controllable in-situ doping and patterning of single-crystal semiconductor nanowires are critical for practical device applications.

In this work, we report the MOCVD growth of undoped and Ga-doped ZnO nanotips on silicon and SOS substrates. Structural and optical properties of the as-grown ZnO nanotips have been investigated.

(Received Sept. 17, 2003; accepted Dec. 1, 2003)

EXPERIMENTAL

The ZnO nanotips were grown on n-type Si and SOS substrates using a vertical flow MOCVD system at low pressure. The Si layer is n-type with (100) orientation, and the sapphire substrate is $(01\bar{1}2)$ r-sapphire. Diethylzinc, oxygen, and triethylgallium were used as the Zn metal-organic source, oxidizer, and Ga-doping source, respectively. Argon was the carrier gas. The growth temperature of ZnO nanotips was in the range of 400–500°C. The growth rate was 1–2 μm/h. The details of the ZnO nanotip growth using MOCVD were described elsewhere.[6] The Ga/Zn mole ratio ranged from 10^{-4} -10^{-2} during the Ga-doped ZnO nanotip growth. Epitaxial ZnO films were simultaneously grown on $(01\bar{1}2)$ r-sapphire[10] substrates during the growth of ZnO nanotips on silicon substrates, serving as reference samples for the comparison of different Ga-doping levels in ZnO nanotips. The resistivities of the reference epitaxial-ZnO films were measured using the four-point-probe method.

A Leo–Zeiss (Oberkocher, Germany), field-emission scanning electron microscope (FESEM) was used to inspect the shape and geometry of the nanotips. A Topcon (Paramus, NJ) 002B transmission electron microscope (TEM) was used to perform detailed structural characterizations. Photoluminescence (PL) spectra were excited with a 325-nm-line He-Cd laser. An optical cryostat was used for the low-temperature PL measurement. The ZnO nanotips were patterned using photolithography and wet-chemical etching. Photoresist served as the etching mask. A NH_4OH and H_2O_2 mixture solution was used to etch ZnO nanotips grown on the Si substrate.

RESULTS AND DISCUSSION

Figure 1a shows a FESEM picture of ZnO nanotips grown on the Si substrate. The ZnO nanotips are very dense and predominatingly oriented along the c-axis with uniform size. The nanotip bottom diameter is in the range of 40–60 nm, and the nanotip length is ~500 nm, giving an aspect ratio of ~10:1. Such nanotip growth is also achieved on SOS substrates. Shown in Fig. 2 is the SEM picture of ZnO nanotips grown on the (100) Si surface of a SOS substrate. The inset of Fig. 2 is the top view of the ZnO nanotips. The ZnO nanotips are found to be preferably c-oriented and terminating with sharp tips. Figure 3 shows patterned ZnO nanotips on a silicon substrate.

X-ray diffraction (XRD) measurements were employed to characterize the crystalline orientation of the ZnO nanotips grown on Si substrates. As shown in Fig. 4a, only the (0001) ZnO peak is present in the x-ray scan, indicating a preferred c-axis orientation. Figure 4b is the selected-area electron diffraction pattern along the $(21\bar{1}0)$ zone axis from the TEM measurement. It confirms that the as-grown ZnO nanotips are single crystalline.

It has been reported that the possible growth mechanisms for 1-D ZnO nanostructures include

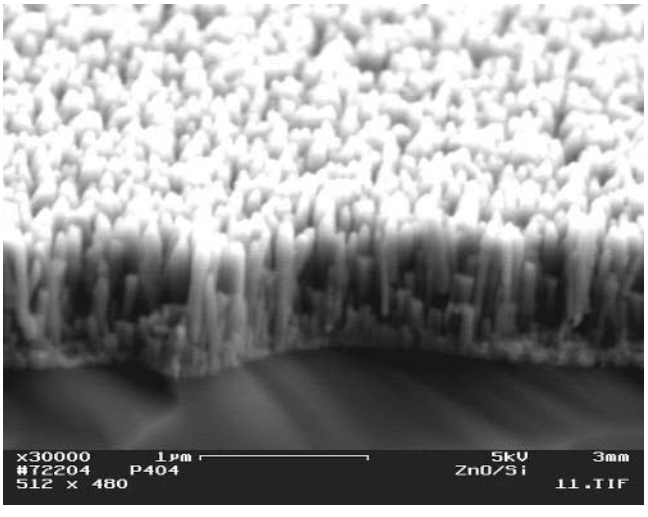

Fig. 1. (a) The FESEM image of ZnO nanotips grown on a Si substrate.

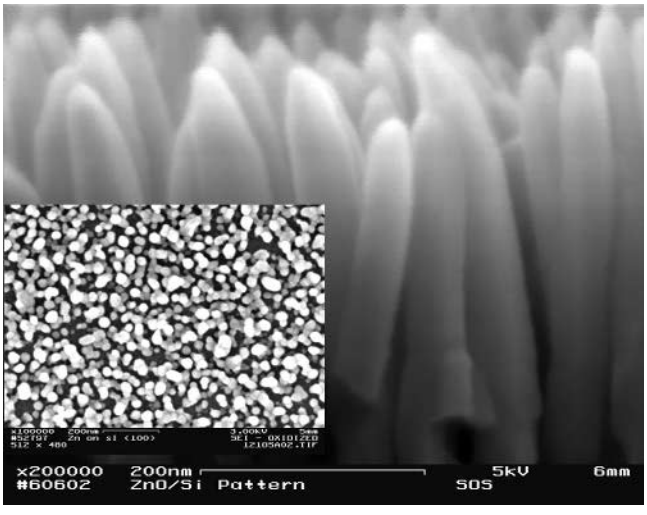

Fig. 2. The FESEM image of ZnO nanotips grown on a SOS substrate. The inset is a top view of ZnO nanotips.

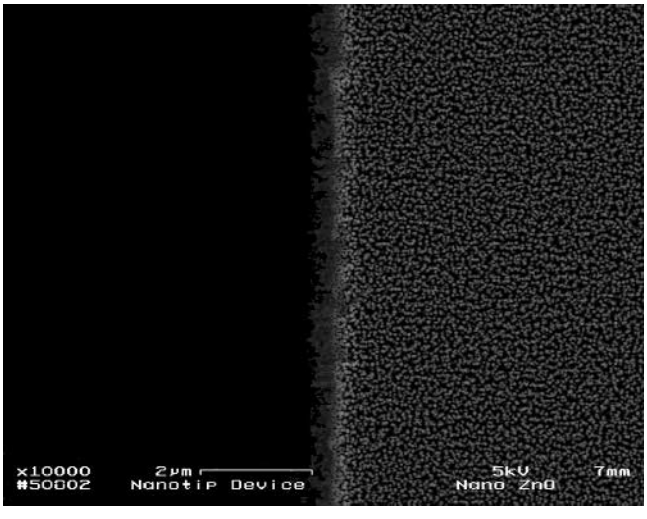

Fig. 3. Patterned ZnO nanotips on a Si substrate.

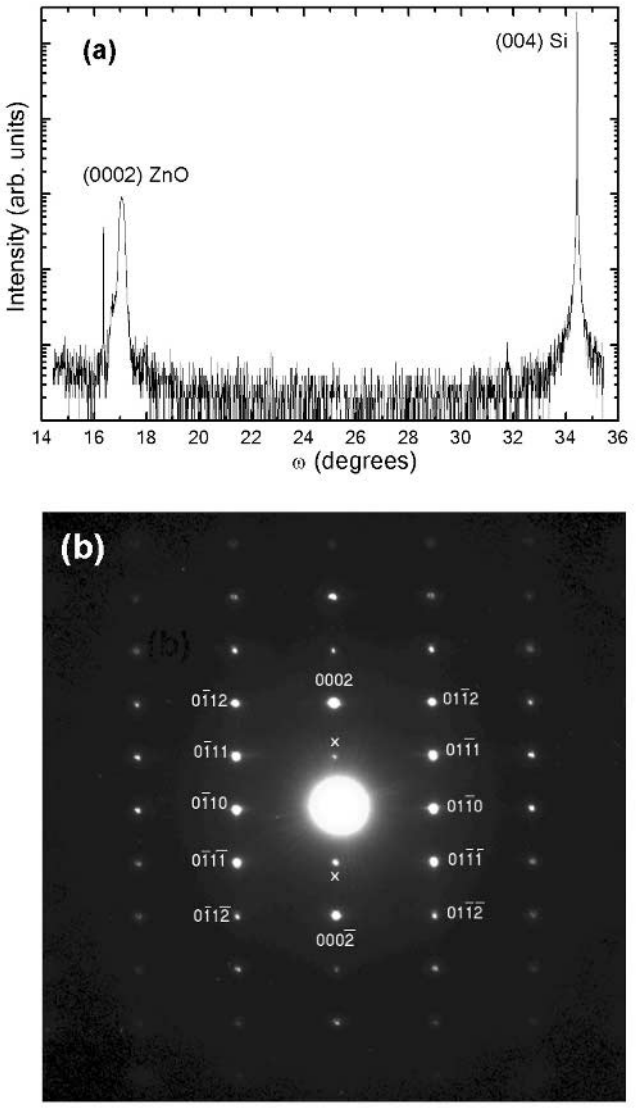

Fig. 4. (a) The XRD pattern of ZnO nanotips grown on a silicon substrate and (b) selected-area diffraction pattern of the ZnO nanotip.

the VLS mechanism,[7,11] screw dislocation growth,[12] catalyst-free self-nucleation growth,[4] and the vapor-solid mechanism.[13,14] ZnO nanotip growth using MOCVD does not require pre-deposition of a metal catalyst onto the substrate surface. We consider that the formation of ZnO nanotips on Si is governed by a catalyst-free self-nucleation process. ZnO is a polar semiconductor, with (0001) planes being Zn-terminated and $(000\bar{1})$ planes being O-terminated. These two crystallographic planes have opposite polarity, thus different surface energies. The growth rate relationship for different ZnO crystal faces is R<0001> >R<$10\bar{1}1$>>R<$(10\bar{1}0)$>, where R is the growth rate. Thus, ZnO has the highest growth rate along its c-axis. A thin SiO_2 layer is formed at the Si and ZnO interface during the initial growth. The ZnO crystals nucleate on the as-formed amorphous SiO_2 layer. As the growth rate is more favored along the c-axis, the self-assembled nanotip growth proceeds.

Figure 5a and curve 1 in Fig. 5b are 77-K and room-temperature PL spectrum of undoped ZnO nanotips grown on a Si substrate, respectively. At room temperature, ZnO nanotips exhibit strong near-band edge emission with negligible deep-level emission. The 77-K PL spectrum of the undoped ZnO nanotips has a dominant peak at 3.37 eV, which can be attributed to the free excitonic transition, in agreement with the previous reports on ZnO nanowires.[5,15] For ZnO nanowires, the dominance of free exciton emission is rarely observed in a low-temperature PL spectrum.[15,16] This is presumably due to the localization of the free excitons by intrinsic defects and impurities. Bound-exciton transitions, mostly donor related, dominate the emission spectra, which primarily result from a high-background carrier concentration. The presence of the dominant, free excitonic emission indicates the high purity and low defect density of ZnO nanotips grown on Si substrates using MOCVD.

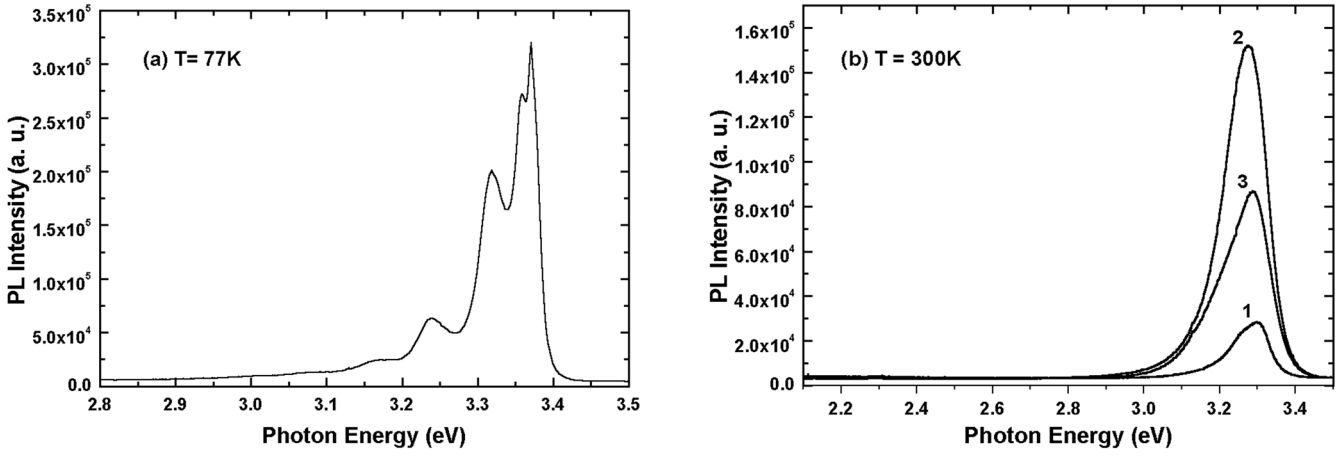

Fig. 5. (a) The 77-K PL spectrum of undoped ZnO nanotips grown on a Si substrate and (b) room-temperature PL spectra of undoped and Ga-doped ZnO nanotips grown on Si substrates. Curve 1 corresponds to the undoped ZnO nanotips with a reference resistivity of 40 Ωcm; curves 2 and 3 correspond to Ga-doped ZnO nanotips with reference resistivities of 4×10^{-3} Ωcm and 3×10^{-3} Ωcm, respectively.

The second strong peak at 3.36 eV in Fig. 5a, with a slightly lower energy than the free exciton emission, is related to bound-exciton emission involving a neutral donor-like complex. Additionally, a PL transition at 3.32 eV is observed. Such a feature has been reported in ZnO nanowires and rods grown on sapphire substrates.[15,16] It could be assigned to the bound-exciton emission arising from free-to-bound transition or to recombination caused by a donor-acceptor pair. It is also noted that up to three longitudinal-optical phonon replicas can be observed at the low energy tail of the 3.32-eV peak.

Figure 5b also shows the room-temperature PL spectra of Ga-doped ZnO nanotips in comparison with the undoped one. Curve 1 is for the undoped ZnO nanotips with a reference resistivity of 40 Ωcm, while curves 2 and 3 correspond to Ga-doped ZnO nanotips with reference resistivities of 4×10^{-3} Ωcm and 3×10^{-3} Ωcm, respectively. For ZnO nanotips, the near-band edge recombination increases when the reference resistivity decreases from 40 Ωcm to 4×10^{-3} Ωcm (curves 1 and 2 in Fig. 5b). With a further increase in the Ga-doping level, the peak intensity decreases (curve 3 in Fig. 5b). Such doping-related PL behavior has been reported in Ga-doped ZnO epitaxial films,[17,18] where a Ga donor-bound exciton complex has been suggested to be responsible for the increase of PL intensity caused by Ga doping. At low or moderate Ga doping levels, the increase in PL intensity in Ga-doped ZnO nanotips arises from a Ga donor-related impurity band emission. At a high Ga-doping level, impurity complexes or clusters could form in the ZnO nanotips. The competition between radiative and nonradiative transitions becomes prominent, resulting in PL quenching.

CONCLUSIONS

We have demonstrated the MOCVD growth of ZnO nanotips on silicon and SOS substrates. The ZnO nanotips are single crystal and vertically aligned along the c axis. The ZnO nanotips display strong near-band edge PL emission with negligible deep-level emission. Free excitonic emission dominates the 77-K PL spectrum of the as-grown, undoped ZnO nanotips, confirming the good optical property of the nanotips. The ZnO nanotips can be doped during the MOCVD growth. The increase in PL intensity caused by Ga doping is attributed to impurity band emission. The ZnO nanotips can be patterned on Si and SOS substrates, offering the potential for integration with Si-based devices.

ACKNOWLEDGEMENTS

The authors thank Dr. H.M. Ng, Bell Labs at Murray Hill, for his help with PL measurement and analysis. This work has been supported by the National Science Foundation under Grant No. CCR-0103096.

REFERENCES

1. X. Duan, Y. Huang, Y. Cui, J. Wang, and C.M. Lieber, *Nature* 409, 66 (2001).
2. M.H. Huang, S. Mao, H. Feick, H.Q. Yan, Y.Y. Wu, H. Kind, E. Weber, R. Russo, and P.D. Yang, *Science* 292, 1897 (2001).
3. Y.W. Heo, V. Varadarajan, M. Kaufman, K. Kim, D.P. Norton, F. Ren, and P.H. Fleming, *Appl. Phys. Lett.* 81, 3046 (2002).
4. J. Wu and S. Liu, *J. Phys. Chem. B* 106, 9546 (2002).
5. W.I. Park, Y.H. Jun, S.W. Jung, and G.-C. Yi, *Appl. Phys. Lett.* 82, 964 (2003).
6. S. Muthukumar, H. Sheng, J. Zhong, Z. Zhang, N.W. Emanaetoglu, and Y. Lu, *IEEE Trans. Nanotechnol.* 2, 50 (2003).
7. M.H. Huang, Y. Wu, H. Feick, N. Tran, E. Weber, and P. Yang, *Adv. Mater.* 13, 113 (2001).
8. L. Dong, J. Jiao, D.W. Tuggle, J.M. Petty, S.A. Elliff, and M. Coulter, *Appl. Phys. Lett.* 82, 1096 (2003).
9. W.I. Park, G. Yi, M. Kim, and S.J. Pennycook, *Adv. Mater.* 14, 1841 (2002).
10. C.R. Gorla, W.E. Mayo, S. Liang, and Y. Lu, *J. Appl. Phys.* 87, 3736 (2000).
11. R.S. Wagner and W.C. Ellis, *Appl. Phys. Lett.* 4, 89 (1964).
12. C.M. Drum and J.W. Mitchell, *Appl. Phys. Lett.* 4, 164 (1964).
13. G.W. Sears, *Acta Met.* 4, 361 (1955).
14. Z.L. Wang, *Adv. Mater.* 15, 432 (2003).
15. Q.X. Zhao, M. Willander, R.E. Morjan, Q.H. Hu, and E.E.B. Campbell, *Appl. Phys. Lett.* 83, 165 (2003).
16. B.P. Zhang, N.T. Binh, Y. Segawa, K. Wakatsuki, and N. Usami, *Appl. Phys. Lett.* 83, 1635 (2003).
17. H.J. Ko, Y.F. Chen, S.K. Hong, H. Wenisch, T. Yao, and D.C. Look, *Appl. Phys. Lett.* 77, 3761 (2000).
18. H. Kato, M. Sano, K. Miyamoto, and T. Yao, *J. Cryst. Growth* 237–239, 538 (2002).